Cardiac Imaging

Diagnostic Value of Contrast-Enhanced Magnetic Resonance Imaging and Single-Photon Emission Computed Tomography for Detection of Myocardial Necrosis Early After Acute Myocardial Infarction

Tareq Ibrahim, MD,* Hubertus P. Bülow, MD,† Thomas Hackl, MD,† Mira Hörnke, MD,†
Stephan G. Nekolla, PHD,† Martin Breuer, MD,* Albert Schömig, MD,*
Markus Schwaiger, MD, FACC†

München, Germany

Objectives   This study sought to evaluate the diagnostic value of contrast-enhanced magnetic resonance imaging (CMR) and single-photon emission computed tomography (SPECT) for detection of myocardial necrosis after acute myocardial infarction (AMI).

Background   Single-photon emission computed tomography is widely accepted in the clinical setting for detection and estimation of myocardial infarction. Contrast-enhanced magnetic resonance imaging offers technical advantages and is therefore a promising new method for identification of infarcted tissue.

Methods   Seventy-eight patients with AMI were examined by CMR and SPECT 7 days after percutaneous coronary intervention. Contrast-enhanced magnetic resonance imaging and SPECT images were scored for presence and location of infarction using a 17-segment model. Results were compared with the peak troponin T level, electrocardiographic, and angiographic findings.

Results   Acute myocardial infarction was detected significantly more often by CMR than SPECT (overall sensitivity: 97% vs. 87%; p = 0.008). Sensitivity of CMR was superior to SPECT in detecting small infarction as assessed by the peak troponin T level <3.0 ng/ml (92 vs. 69%; p = 0.03), and infarction in non-anterior location (98% vs. 84%; p = 0.03). Non–Q-wave infarctions were more likely to be detected by CMR (sensitivity 85% vs. 46%; p = 0.06). While CMR offered high sensitivity for detection of AMI irrespective of the infarct-related artery, SPECT was less sensitive, particularly within the left circumflex artery territory.

Conclusions   Contrast-enhanced magnetic resonance imaging is superior to SPECT in detecting myocardial necrosis after reperfused AMI because CMR detects small infarcts that were missed by SPECT independent of the infarct location. Thus, CMR is attractive for accurate detection and assessment of the myocardial infarct region in patients early after AMI.   (J Am Coll Cardiol 2007;49:208–16) © 2007 by the American College of Cardiology Foundation

Reperfusion therapy has significantly reduced mortality in patients with acute myocardial infarction (AMI) (1). However, use of mortality as an end point to demonstrate advantages of new reperfusion strategies requires large numbers of patients (2). Thus, there is growing interest in markers that can be used as surrogate for mortality in trials assessing the efficacy of reperfusion therapy. It has been shown, that the extent and degree of irreversible myocardial tissue injury after AMI are strong predictors of patient outcome, and interventions that reduce injury significantly improve prognosis (3). Nuclear imaging techniques such as single-photon emission computed tomography (SPECT) using ^{99m}Tc-sestamibi as a tracer are currently widely used in the clinical practice for the detection and estimation of myocardial infarction (MI) after reperfusion therapy and to predict outcome according to infarct size (2,4) or myocardial salvage (5). However, technical limitations of SPECT imaging such as a low spatial resolution may impair delineation of small infarcts in up to 25% of patients with AMI

(2,4). Because modern reperfusion therapies constantly improve and smaller infarcts are more frequently to be expected, this amount may even increase in the future. Furthermore, regional relative tracer inhomogenities resulting from soft tissue attenuation or scatter may compromise the diagnostic accuracy of SPECT imaging (6,7).

Findings from several studies have indicated that contrast-enhanced magnetic resonance imaging (CMR) enables the visualization of AMI and documentation of reperfusion with high spatial resolution (8–13). In a previous study, we have validated measures of CMR enhancement in patients with rather large AMI in comparison with quantitative SPECT imaging and shown a high correlation for estimation of infarct size (14). So far, there are only a few reports comparing the diagnostic value of CMR with that of SPECT in terms of infarct detection. In old MI, it has been recently shown that CMR can detect subendocardial infarcts that are missed by SPECT (15). Further data in patients with AMI suggest that CMR may be superior to SPECT for detecting small infarcts in the inferior wall (16). In this study, we sought to investigate the diagnostic value of CMR and SPECT for the detection of myocardial necrosis in patients early after AMI and reperfusion therapy.

Methods

Patients. During a 2-year period (March 2002 to March 2004), we consecutively enrolled 78 patients with AMI (onset of symptoms <48 h). Diagnosis of AMI was based on the presence of chest pain lasting at least 20 min associated with electrocardiographic (ECG) changes (ST-segment elevation or depression, pathologic Q waves, left bundle branch block of new onset) and elevation of troponin T activity (>0.1 ng/ml) (17). A total of 164 patients were screened for inclusion into the study. Patients were excluded for the following reasons: prior infarction (n = 17), death (n = 10), no scintigraphy (n = 21), claustrophobia (n = 12), reject consent (n = 16), pacemaker (n = 4), technical reason (n = 6). Patients from our previous study were all included (14). On the day of admission, all patients underwent coronary angiography with percutaneous coronary intervention (n = 75 stenting; n = 3 angioplasty) of the infarct-related artery. Contrast-enhanced magnetic resonance imaging and SPECT were performed in all patients median (25th, 75th percentiles), 7.0 (6.0, 8.0) days after infarction. The study protocol was reviewed and approved by the local ethics committee. Written informed consent was obtained before inclusion in the study.

Protocol. Contrast-enhanced magnetic resonance imaging was performed on a 1.5-T tomograph (Siemens Sonata, Erlangen, Germany) equipped with a dedicated cardiac phased-array surface coil. All images were obtained in repeated breath hold and were gated to the ECG. Contiguous short-axis slices and representative long-axis slices of the left ventricle (LV) were acquired 20 min after intravenous bolus injection of 0.2 mmol/kg gadolinium-diethlenetriamine pentaacetic acid

(Gd-DTPA) (Magnevist, Schering AG, Berlin, Germany). Between March 2002 and April 2003, a segmented inversion-recovery TrueFISP-sequence was used (slice thickness 8 mm, repetition time (TR) 2.3 ms, echo time (TE) 1.4 ms, image matrix 256 × 256, flip angle 60°; n = 40 patients). Thereafter, CMR was performed using a 3-dimensional segmented inversion-recovery TurboFLASH-sequence (slice thickness 4 mm, TR 4.0 ms, TE 1.5 ms, image matrix 256 × 256, flip angle 30°; n = 38 patients). The inversion time was individually chosen to null normal myocardium.

Single-photon emission computed tomography imaging was performed after intravenous injection of 350 MBq technetium-99m-sestamibi using a camera system (MultiSPECT 3, Siemens AG, Erlangen, Germany) equipped with low-energy, parallel-hole collimators. Images were acquired ECG-gated in a 64 × 64 data matrix with an acquisition time of 40 s/projection. Summed data were reconstructed over 180° from 45° right anterior oblique to 45° left posterior oblique by use of a Butterworth filter and were realigned to generate short- and long-axis views.

Image analysis. Contrast-enhanced magnetic resonance imaging and SPECT were compared using a 17-segment model as previously recommended by the American Heart Association (18). Based on this model, representative short-axis slices of the basal (6 segments), mid-ventricular (6 segments), and apical (4 segments) region of the LV were analyzed. The apex was evaluated from long-axis slices. A total of 1,326 segments were assessed for both CMR and SPECT using semiquantitative scores.

For CMR, the presence or absence of contrast enhancement (CE) as well as the transmural extent of CE within each segment was defined visually and subjectively by 2 blinded observers by consensus according to the following scheme: 0 = no enhancement, 1 = 1% to 25%, 2 = 26% to 50%, 3 = 51% to 75%, 4 = 76% to 100% enhancement extent referred to the myocardial wall thickness (15). Single-photon emission computed tomography images were interpreted by an experienced nuclear cardiologist who was blinded to the clinical data and the CMR results. Segments were scored from 0 to 4: 0 = normal perfusion, 1 = mildly reduced, 2 = moderately reduced, 3 = severely reduced, 4 = absent tracer activity (19). For both modalities, a score of ≥1 in at least 1 segment was defined as abnormal. Regional assessment of CMR and SPECT was performed within 234 corresponding vascular territories. Segments were generally assigned to 1 of the 3 major coronary arteries

Table 1	Patient Characteristics
Age (yrs)	63.9 (53.8, 71.7)
Female gender (%)	23.1
Arterial hypertension (%)	79.5
Diabetes mellitus (%)	19.2
Current smoker (%)	35.9
Hypercholesterolemia (%)	69.2
Prior angioplasty (%)	2.6
Prior CABG (%)	3.8
Infarct location (%)	
Anterior	44.9
Lateral	14.1
Inferior	41.0
ECG (%)	
Q-wave infarction	83.3
Non–Q-wave infarction	16.7
Killip class (%)	
1	79.4
2	16.7
3	1.3
4	2.6
Peak troponin T (ng/ml)	3.9 (2.2, 8.1)
Severity of coronary artery disease (%)	
Single-vessel disease	35.8
Two-vessel disease	32.1
Three-vessel disease	32.1
Ejection fraction before angioplasty (%)	52.5 (45.0, 58.0)
Infarct-related artery (n)	
LAD	35
LCX	14
RCA	30
Final TIMI flow grade (%)	
0	0
1	1.3
2	6.4
3	92.3

CABG = coronary artery bypass grafting; LAD = left anterior descending coronary; LCX = left circumflex artery; RCA = right coronary artery; TIMI = Thrombolysis In Myocardial Infarction.

(18). The individual coronary anatomy and the infarct-related artery were determined by an experienced physician reading the coronary angiogram.

Statistical analysis. All results are expressed as median (25th, 75th percentiles). Sensitivity of CMR and SPECT was determined for the detection of myocardial necrosis. Non-accordance was tested with the McNemar test. The 2-tailed Fisher exact test and non-parametric test (Mann-Whitney, Wilcoxon) were used for comparison of categoric and continuous variables. A value of p < 0.05 was considered statistically significant.

Results

Patient and infarct characteristics. Demographic, clinical, and angiographic characteristics of the patients are shown in Table 1. Two patients had prior coronary angioplasty, and 3 patients had coronary bypass surgery at least 6 months before study inclusion. Peak troponin T in all patients ranged from 0.38 to 17.90 ng/ml. One patient angiographically displayed occlusion of the left anterior descending artery (LAD) and left circumflex artery (LCX), and AMI was related to both vessels.

Detection of MI. Examples of CMR and SPECT imaging in patients with AMI are shown in Figure 1. Overall sensitivity of CMR and SPECT for the detection of MI was 97% and 87%, respectively (p = 0.008). Two of 78 patients showed no CE by CMR. These patients were examined each with one of both magnetic resonance sequences and also had a normal SPECT study. Myocardial infarction in those patients was small as assessed by the peak troponin T level (1.37 and 1.40 ng/ml). However, SPECT failed to detect AMI in 10 of 78 patients. Infarcts missed by SPECT were significantly smaller than those that were detected as assessed by the peak troponin T level (1.4 [0.5, 2.4] vs. 4.5 [2.7, 8.7] ng/ml; p < 0.001), and small MI as defined by the peak troponin T level was significantly more often detected by CMR than by SPECT (Fig. 2A).

Comparison with ECG findings. The 2 patients with normal CMR study showed non–Q-wave infarction within the anterior and inferior region. Infarcts missed by SPECT were localized anterior (n = 3), lateral (n = 3), and inferior (n = 4). The sensitivity of CMR and SPECT for the detection of anterior infarction was 97% and 91%, respectively (p = 0.5). While the detection of infarction in a non-anterior location was also high by CMR (98%), SPECT was significantly less sensitive within this region (84%; p = 0.03) (Fig. 2B).

The overall sensitivity for the detection of Q-wave infarction by CMR and SPECT was 100% and 95%, respectively (Fig. 2C). Identification of Q-wave infarction was high for both modalities independent of the infarct location (Table 2). However, non–Q-wave infarction was detected by CMR in 11 of 13 patients, but only in 6 of 13 patients by SPECT. The sensitivity for CMR and SPECT to detect non–Q-wave infarction was 85% and 46%, respectively (p = 0.06). Patients with a normal SPECT study had significantly more often non–Q-wave infarction (70%; 7 of 10) compared with those patients with perfusion defect (9%; 6 of 68) (p < 0.001). Although the number of patients with non–Q-wave infarction was low in this study, there was a clear trend that CMR detected these infarcts more often than SPECT in a non-anterior location (Table 2, Fig. 3).

Comparison with angiographic findings. Regional analysis according to the major coronary artery supply showed a high sensitivity for CMR to detect MI independent of the infarct-related artery (Fig. 4). The sensitivity for CMR in the LAD, LCX, and right coronary artery (RCA) region was 97%, 100%, and 97%, respectively. Sensitivity of SPECT was lower in all vascular regions compared with CMR. The sensitivity of SPECT to detect MI within the LAD and RCA was 89% and 87%, respectively. However, SPECT displayed the lowest sensitivity for the detection of infarction within the LCX territory (79%). Although re-
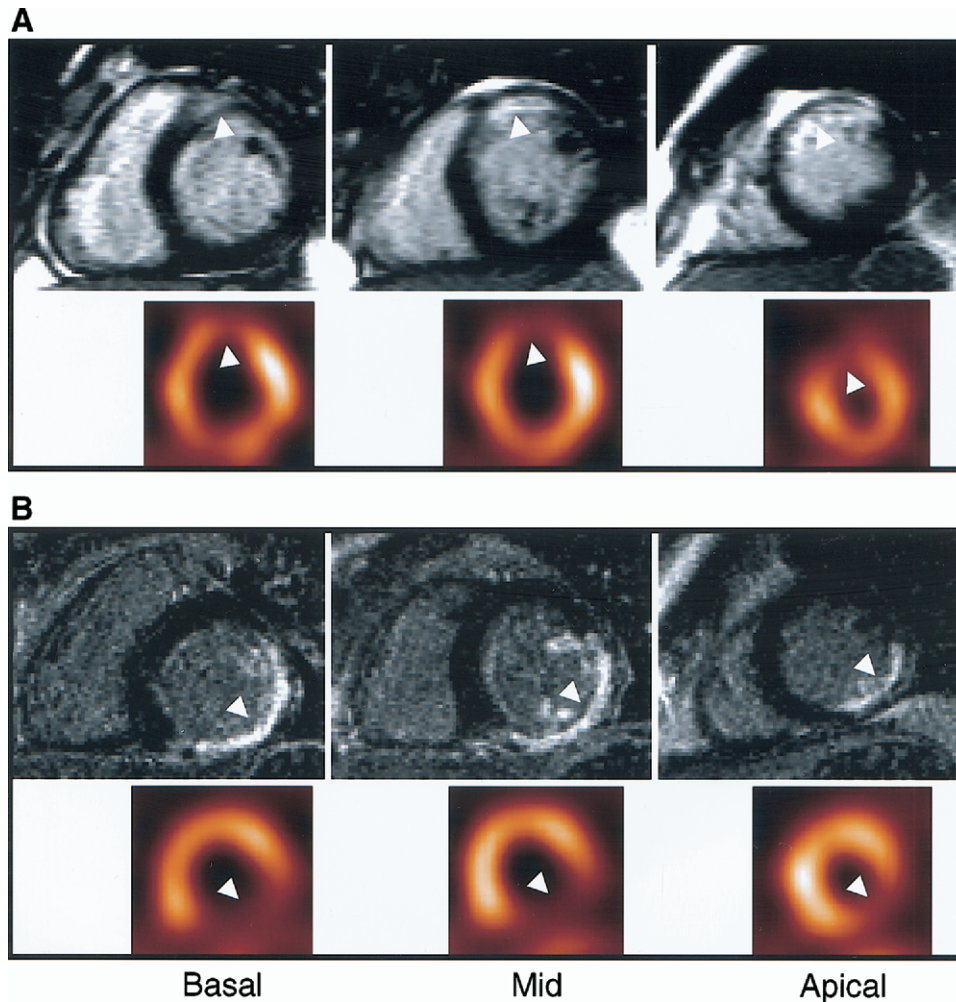
Figure 1   **Comparison of CMR and SPECT**

(A) Non-transmural enhancement by contrast-enhanced magnetic resonance imaging (CMR) **(upper row, arrows)** in the anterior and antero-septal region (score 2 to 3) (TrueFISP sequence) with corresponding perfusion defect by single-photon emission computed tomography (SPECT) **(lower row, arrows)**. **(B)** Transmural enhancement by CMR **(upper row, arrows)** in the inferior region (score 3 to 4) and non-transmural enhancement in the lateral region (score 2 to 3) (TurboFLASH sequence) with corresponding perfusion defect by SPECT **(lower row, arrows)**.

gional comparison of CMR and SPECT showed a clear trend that CMR revealed higher sensitivity in all vascular territories, this was not statistically significant.

Two patients with a LAD-related infarction had CE within regions assigned to both the LAD and LCX territory. One patient with a LAD-related infarction and 5 patients with an LCX-related infarction had an extension of perfusion defect by SPECT including both the LAD and the LCX region. However, 7 patients with a LAD-related infarction showed an additional hypoperfusion within the RCA territory by SPECT imaging, which was regarded as false positive (Fig. 5).

Discussion

The present study indicates that CMR is more sensitive than Tc-99m-sestamibi SPECT in detecting necrotic myo-

cardium in patients early after reperfused AMI, because CMR detects myocardial infarcts irrespective of size and location, while SPECT particularly failed to detect small infarcts in non-anterior regions.

Assessment of reperfused AMI by CMR. Regions of reperfused AMI display a CE on T1-weighted CMR images acquired more than a few minutes after administration of paramagnetic contrast agents. The underlying mechanisms leading to CE are not fully understood. It is thought that cellular degradation in the infarcted region results in an increase in the permeability and enlargement of the extracellular space and, hence, an increased distribution volume for extracellular contrast agents such as Gd-DTPA. Moreover, gadolinium chelats wash out of infarcted tissue more slowly than out of healthy myocardium, which can be visualized by delayed imaging acquisition (18). Although
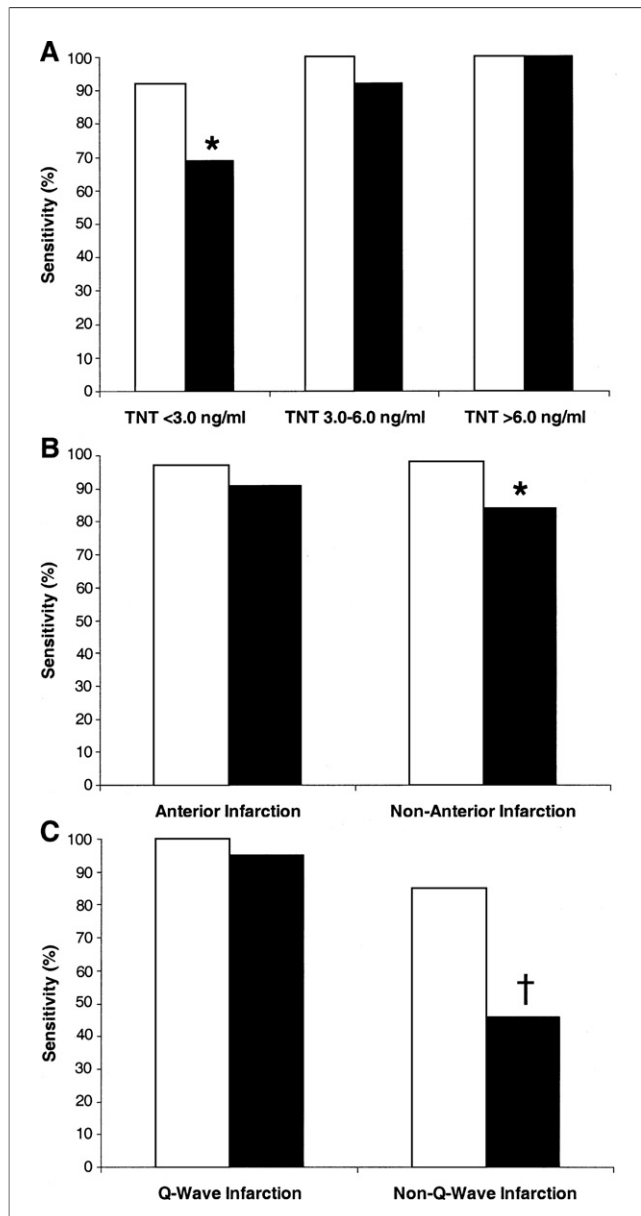
(A) Sensitivity of contrast-enhanced magnetic resonance imaging (CMR) and single-photon emission computed tomography (SPECT) for detection of acute myocardial infarction (AMI) based on the peak troponin T levels (TNT). Groups were defined by peak troponin T level <3.0 ng/ml (n = 26), 3.0 to 6.0 ng/ml (n = 27), and >6.0 ng/ml (n = 25) (*p = 0.03). **(B)** Detection of AMI in anterior and non-anterior regions by CMR and SPECT (*p = 0.03). **(C)** Detection of electrocardiogram defined Q-wave and non–Q-wave infarction by CMR and SPECT (†p = 0.06). **Open bars** = CMR; **solid bars** = SPECT.

Gd-DTPA is non-specific for necrotic myocardium, it has been shown that infarct size can be reliably measured by CMR enhancement after reperfusion in comparison to triphenyl-tetrazolium-chloride staining (9,10,12,20). However, some of the prior studies have shown that CMR slightly overestimates the histopathological infarct size very early after reperfusion (within 48 h) suggesting that tissue edema of reversibly injured tissue at the periphery of the

infarct region may contribute to CE (10,12,13,20). Furthermore, it could be recently demonstrated that the size of enhancement based on a gadolinium contrast agent revealed a decrease within the first 2 days after reperfusion (21). Scintigraphic studies during the acute phase of MI have shown that early imaging is more sensitive than later imaging, particularly if patients received reperfusion therapy (22,23). It is not quite clear why early imaging is more sensitive, but maybe similar factors as described for CE by CMR such as resolution of the peri-infarction edema may be responsible. Because we aimed to assess the detection of the final myocardial necrosis, patients were examined 7 days after AMI and reperfusion by both modalities. This period of time is commonly used in clinical trials aiming for the scintigraphic assessment of the final infarct extent after AMI and reperfusion therapy (24). However, we cannot rule out whether an earlier imaging time point would have increased the diagnostic sensitivity for both CMR and SPECT.

Comparison of CMR and SPECT. In this study, detection of AMI by CMR was superior to SPECT because 13% of all patients displayed a normal SPECT perfusion examination. Other SPECT studies in patients with AMI reported comparable rates of undetected infarcts ranging from 11% to 25% (4,6). Because the spatial resolution of SPECT images is about $10 \times 10 \times 10$ mm and comparable with the thickness of the heart wall, non-transmural infarcts are difficult to detect (22). Conversely, the in-plane resolution of CMR was typically 1.4×1.4 mm, which yields 5 to 10 pixels within the heart wall, making it possible to identify subendocardial infarction. The ability of CMR to detect subendocardial infarction with high sensitivity in comparison with ECG or SPECT has been also reported in patients with chronic MI (15,25).

We further showed that CMR was more sensitive than SPECT in detecting MI in non-anterior locations. A lesser sensitivity of SPECT for inferior MI has been described previously (23,26). It is well known that sensitivity of conventional SPECT may be decreased by degradation of image quality resulting from soft tissue attenuation, compton scatter, or depth-dependent reduction of spatial resolution (7). The low sensitivity of SPECT within the LCX region in our study may be explained by the relatively high tracer activity within the lateral wall due to the close relation

Table 2 Regional Detection of Q-Wave and Non–Q-Wave Infarction by CMR and SPECT

	CMR	SPECT
Anterior infarction		
Q-wave	100% (31/31)	94% (29/31)
Non–Q-wave	75% (3/4)	75% (3/4)
Non-anterior infarction		
Q-wave	100% (34/34)	97% (33/34)
Non–Q-wave	89% (8/9)	33% (3/9)

CMR = contrast-enhanced magnetic resonance imaging; SPECT = single-photon emission computed tomography.
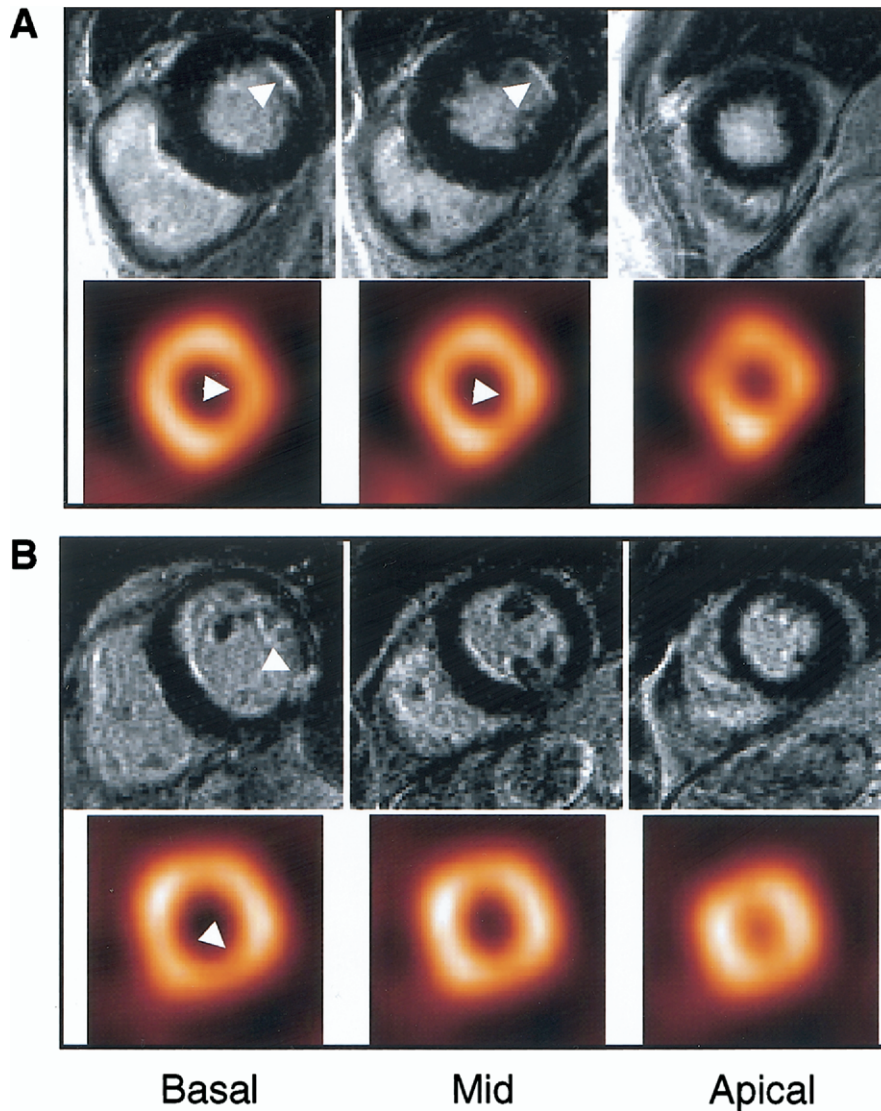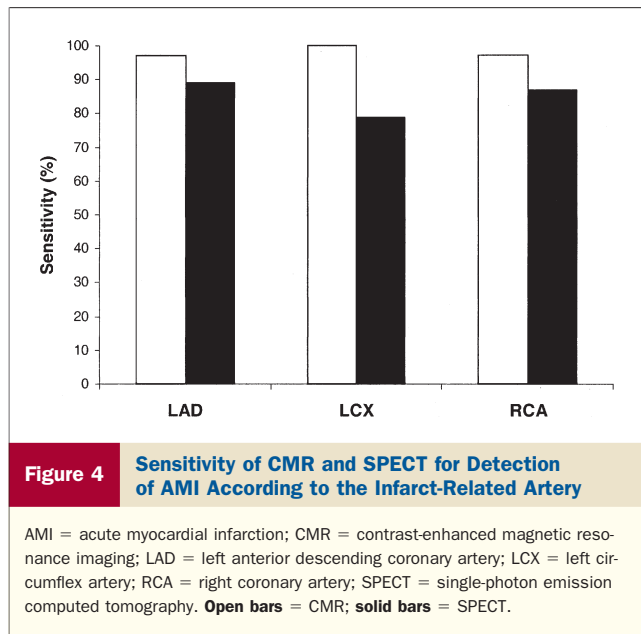
Figure 3   **Discordant CMR and SPECT Results**

Contrast-enhanced magnetic resonance imaging (CMR) enhancement **(arrows)** in **(A)** the subendocardium of the basal and mid-lateral wall (score 1), and **(B)** localized transmural enhancement of the basal inferolateral wall (score 3) with normal single-photon emission computed tomography (SPECT) perfusion imaging **(arrows)**.

to the camera face, which may lead to a visual underestimation of perfusion abnormalities. In addition, localized attenuation by overlying soft tissue or partial volume effect related to regional abnormal wall motion and wall thinning may create artifacts that mimic true perfusion abnormalities and thereby decrease specificity. As observed in some of our patients, the occurrence of false-positive defects in the inferior region is a well-known phenomenon for thallium-201 SPECT imaging (27). Although artifacts are reduced with Tc-99m-sestamibi SPECT due to its favorable properties, false-positive results range from 14% to 38% (28,29). A variety of indirect measures and several attenuation correction solutions have been proposed as methods to reduce the impact of attenuation and partial volume effect in

SPECT imaging (7). For example, transmission image acquisition increased the normalcy rate for visual analysis in patients with coronary artery disease due to a marked improvement in specificity (from 46% to 82%), particularly within the RCA region (30). However, all methods have limitations, and no clinical study have shown significant improvement in sensitivity of SPECT with attenuation correction (7). Attenuation correction, especially by the new SPECT/computed tomography systems, offers the potential for improved diagnostic accuracy of SPECT but requires a standardized approach to image interpretation.

Clinical implications. There are several reasons why it is important to accurately distinguish between infarcted and non-infarcted myocardium early after AMI. Patients with

Figure 4 | **Sensitivity of CMR and SPECT for Detection of AMI According to the Infarct-Related Artery**

AMI = acute myocardial infarction; CMR = contrast-enhanced magnetic resonance imaging; LAD = left anterior descending coronary artery; LCX = left circumflex artery; RCA = right coronary artery; SPECT = single-photon emission computed tomography. **Open bars** = CMR; **solid bars** = SPECT.

acute ventricular dysfunction primarily resulting from myocardial necrosis have a worse prognosis than patients with reversible ventricular dysfunction (31), and injured but viable myocardium is potentially at risk for future infarction if reperfusion therapy has not been complete and significant stenosis remains (32). Moreover, measurement of infarct size is an attractive surrogate end point instead of mortality for the early assessment of new therapies of AMI.

Single-photon emission computed tomography perfusion imaging has been proven to be a robust and clinically well-validated method that can be quantified by using a standardized approach (33). During the past decade, multiple randomized clinical trials have been performed using Tc-99m-sestamibi infarct size as an end point in predicting outcome after AMI and reperfusion (2). Although magnetic resonance imaging has definite technical advantages compared with SPECT imaging allowing visualization of small infarction that are missed by SPECT, the clinical relevance in patients with elevated biomarkers diagnostic for AMI is questionable. However, CMR provides infarct delineation across the ventricular wall, which predicts long-term improvement of contractile function (34). Contrast-enhanced magnetic resonance imaging infarct size relates directly to long-term prognosis in patients with AMI (35). Because current reperfusion therapies are highly effective and smaller infarctions are the consequence, CMR may have important implications for clinical trials assessing the efficacy of reperfusion strategies.

Myocardial perfusion-CMR using extracellular magnetic resonance contrast agents have recently been shown to allow assessment of severe coronary artery disease in the clinical setting (36). New techniques evaluating magnetic resonance contrast kinetics as markers of myocardial blood flow are promising, but have to be considered experimental. Further studies are necessary to validate magnetic resonance imaging protocols combining evaluation of infarct size and stress-induced ischemia. At the current time, gated SPECT at rest
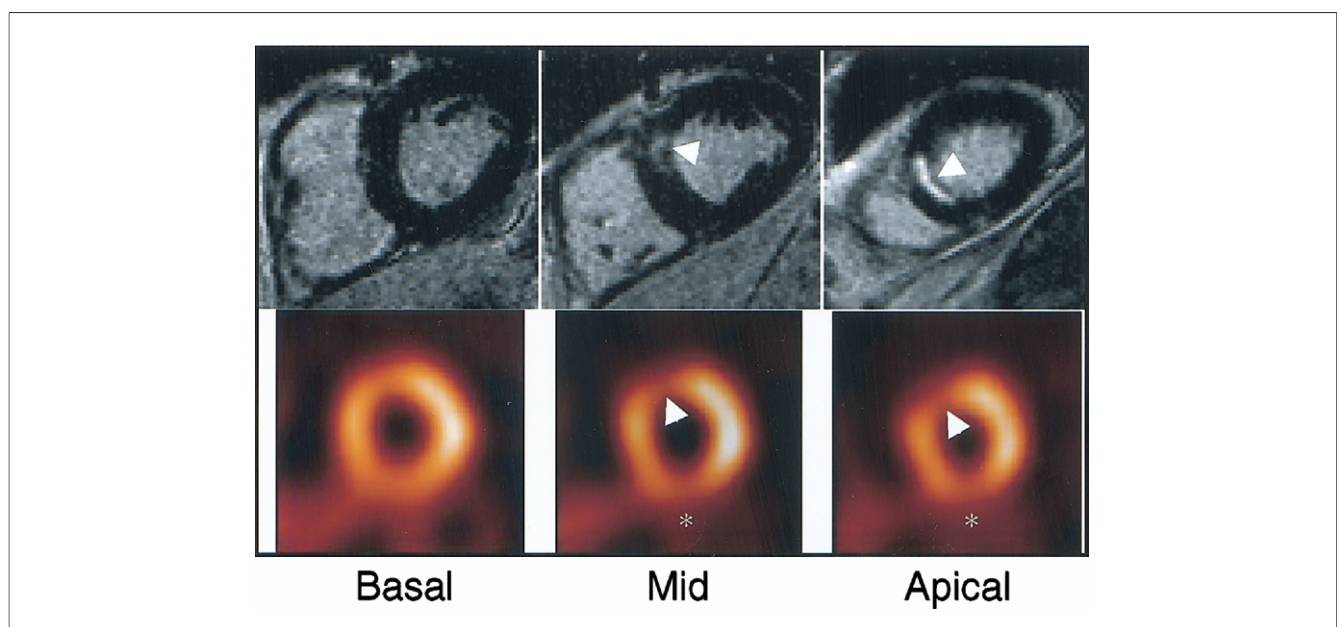

Basal   Mid   Apical

Figure 5 | **Discordant CMR and SPECT Results**

Patient with a left anterior descending coronary artery-related anteroseptal infarction within the mid and apical region with non-transmural enhancement by contrast-enhanced magnetic resonance imaging (CMR) (score 2 to 3) and single-photon emission computed tomography perfusion defect **(arrows)**. However, single-photon emission computed tomography (SPECT) additionally displayed a false positive perfusion defect **(*)** in the inferior wall without corresponding enhancement.

and stress represents the established method to characterize extent and severity of stress-induced ischemia.

Study limitations. In order to assess the diagnostic value of CMR and SPECT for detection of MI, both modalities were compared by a visual semiquantitative analysis. However, we did not evaluate infarct size. Despite publications documenting methods to quantitate the region of hyperenhancement by using different threshold techniques (8,14,37), no standardized approach is so far established to define CMR-infarct size. The visual quantification scheme used for assessment of hyperenhancement in the present study is currently widely accepted to define the transmural extent of MI in clinical magnetic resonance imaging studies (15,25,34).

Because only patients with AMI were included into the study, we only investigated sensitivity. Semiquantitative SPECT analysis was performed using an established score to differentiate between normal and abnormal (19). Because we aimed for the sensitive detection of infarction by SPECT, a score of ≥ 1 was used. However, in some studies, a segmental score ≥ 2 is considered abnormal, which would have decreased overall sensitivity of SPECT from 87% to 72% in this study.

Despite availability of several attenuation correction solutions at the current time, these methods are still under development and evaluation, and no clinical study has shown significant improvement in the sensitivity of SPECT with attenuation correction (7). Thus, attenuation correction was not performed in our study.

Two different magnetic resonance imaging sequences were used in this study. It has been shown that the segmented inversion-recovery TurboFLASH sequence produces a greater difference in regional myocardial signal intensity compared with the TrueFISP sequence (38). However, sensitivity was high for both imaging techniques (97% vs. 98%). Those 2 patients with small infarcts that showed no CE by CMR each were examined with one of both sequences.

Conclusions. The diagnostic value of CMR is superior to SPECT in detecting myocardial necrosis early after AMI because CMR detects small subendocardial infarcts that are missed by SPECT independent of their location. Due to the definite technical advantages of CMR, it may help to overcome well-known limitations of SPECT imaging. Thus, CMR has the potential to accurately assess myocardial infarct size and to serve as a surrogate end point instead of early mortality in clinical trials evaluating the efficacy of reperfusion therapies during the acute setting of infarction. Further studies have to be performed to prove its utility in randomized single- or multicenter trials comparable to the existing evidence of Tc-99m-sestamibi SPECT imaging.

Reprint requests and correspondence: Dr. Tareq Ibrahim, Deutsches Herzzentrum München, Lazarettstr. 36, 80636 München, Germany. E-mail: T.Ibrahim@lrz.tu-muenchen.de.

REFERENCES

1. Gruppo Italiano per lo Studio della Streptochinasi nell'Infarto Miocardico (GISSI). Effectiveness of intravenous thrombolytic treatment in acute myocardial infarction. Lancet 1986;1:397–402.
2. Gibbons RJ, Valeti US, Araoz PA, Jaffe AS. The quantification of infarct size. J Am Coll Cardiol 2004;44:1533–42.
3. Gersh BJ, Anderson JL. Thrombolysis and myocardial salvage. Results of clinical trials and the animal paradigm—paradoxic or predictable? Circulation 1993;88:296–306.
4. Miller TD, Christian TF, Hopfenspirger MR, Hodge DO, Gersh BJ, Gibbons RJ. Infarct size after acute myocardial infarction measured by quantitative tomographic 99mTc sestamibi imaging predicts subsequent mortality. Circulation 1995;92:334–41.
5. Ndrepepa G, Mehilli J, Schwaiger M, et al. Prognostic value of myocardial salvage achieved by reperfusion therapy in patients with acute myocardial infarction. J Nucl Med 2004;45:725–9.
6. Kontos MC, Kurdziel K, McQueen R, et al. Comparison of 2-dimensional echocardiography and myocardial perfusion imaging for diagnosing myocardial infarction in emergency department patients. Am Heart J 2002;143:659–67.
7. Hendel RC, Corbett JR, Cullom SJ, DePuey EG, Garcia EV, Bateman TM. The value and practice of attenuation correction for myocardial perfusion SPECT imaging: a joint position statement from the American Society of Nuclear Cardiology and the Society of Nuclear Medicine. J Nucl Cardiol 2002;9:135–43.
8. Kim RJ, Chen EL, Lima JA, Judd RM. Myocardial Gd-DTPA kinetics determine MRI contrast enhancement and reflect the extent and severity of myocardial injury after acute reperfused infarction. Circulation 1996;94:3318–26.
9. Kim RJ, Fieno DS, Parrish TB, et al. Relationship of MRI delayed contrast enhancement to irreversible injury, infarct age, and contractile function. Circulation 1999;100:1992–2002.
10. Schaefer S, Malloy CR, Katz J, et al. Gadolinium-DTPA-enhanced nuclear magnetic resonance imaging of reperfused myocardium: identification of the myocardial bed at risk. J Am Coll Cardiol 1988;12:1064–72.
11. Lima JA, Judd RM, Bazille A, Schulman SP, Atalar E, Zerhouni EA. Regional heterogeneity of human myocardial infarcts demonstrated by contrast-enhanced MRI. Potential mechanisms. Circulation 1995;92:1117–25.
12. Judd RM, Lugo-Olivieri CH, Arai M, et al. Physiological basis of myocardial contrast enhancement in fast magnetic resonance images of 2-day-old reperfused canine infarcts. Circulation 1995;92:1902–10.
13. Rochitte CE, Lima JA, Bluemke DA, et al. Magnitude and time course of microvascular obstruction and tissue injury after acute myocardial infarction. Circulation 1998;98:1006–14.
14. Ibrahim T, Nekolla SG, Hornke M, et al. Quantitative measurement of infarct size by contrast-enhanced magnetic resonance imaging early after acute myocardial infarction: comparison with single-photon emission tomography using Tc99m-sestamibi. J Am Coll Cardiol 2005;45:544–52.
15. Wagner A, Mahrholdt H, Holly TA, et al. Contrast-enhanced MRI and routine single photon emission computed tomography (SPECT) perfusion imaging for detection of subendocardial myocardial infarcts: an imaging study. Lancet 2003;361:374–9.
16. Lund GK, Stork A, Saeed M, et al. Acute myocardial infarction: evaluation with first-pass enhancement and delayed enhancement MR imaging compared with 201Tl SPECT imaging. Radiology 2004;232:49–57.
17. Alpert JS, Thygesen K, Antman E, Bassand JP. Myocardial infarction redefined—a consensus document of the Joint European Society of Cardiology/American College of Cardiology Committee for the Redefinition of Myocardial Infarction. J Am Coll Cardiol 2000;36:959–69.
18. Cerqueira MD, Weissman NJ, Dilsizian V, et al. Standardized myocardial segmentation and nomenclature for tomographic imaging of the heart: a statement for healthcare professionals from the Cardiac

Imaging Committee of the Council on Clinical Cardiology of the American Heart Association. Circulation 2002;105:539–42.

19. American Society of Nuclear Cardiology. Imaging guidelines for nuclear cardiology procedures, part 2. J Nucl Cardiol 1999;6:G47–84.

20. Goldman MR, Brady TJ, Pykett IL, et al. Quantification of experimental myocardial infarction using nuclear magnetic resonance imaging and paramagnetic ion contrast enhancement in excised canine hearts. Circulation 1982;66:1012–6.

21. Saeed M, Lund G, Wendland MF, Bremerich J, Weinmann H, Higgins CB. Magnetic resonance characterization of the peri-infarction zone of reperfused myocardial infarction with necrosis-specific and extracellular nonspecific contrast media. Circulation 2001;103:871–6.

22. Wackers FJ, Sokole EB, Samson G, et al. Value and limitations of thallium-201 scintigraphy in the acute phase of myocardial infarction. N Engl J Med 1976;295:1–5.

23. Gibbons RJ, Verani MS, Behrenbeck T, et al. Feasibility of tomographic 99mTc-hexakis-2-methoxy-2-methylpropyl-isonitrile imaging for the assessment of myocardial area at risk and the effect of treatment in acute myocardial infarction. Circulation 1989;80:1277–86.

24. Schömig A, Kastrati A, Dirschinger J, et al. Coronary stenting plus platelet glycoprotein IIb/IIIa blockade compared with tissue plasminogen activator in acute myocardial infarction. Stent versus Thrombolysis for Occluded Coronary Arteries in Patients with Acute Myocardial Infarction Study Investigators. N Engl J Med 2000;343:385–91.

25. Wu E, Judd RM, Vargas JD, Klocke FJ, Bonow RO, Kim RJ. Visualisation of presence, location, and transmural extent of healed Q-wave and non–Q-wave myocardial infarction. Lancet 2001;357:21–8.

26. Heller GV, Stowers SA, Hendel RC, et al. Clinical value of acute rest technetium-99m tetrofosmin tomographic myocardial perfusion imaging in patients with acute chest pain and nondiagnostic electrocardiograms. J Am Coll Cardiol 1998;31:1011–7.

27. DePuey EG, Garcia EV. Optimal specificity of thallium-201 SPECT through recognition of imaging artifacts. J Nucl Med 1989;30:441–9.

28. Hendel RC, Berman DS, Cullom SJ, et al. Multicenter clinical trial to evaluate the efficacy of correction for photon attenuation and scatter in SPECT myocardial perfusion imaging. Circulation 1999;99:2742–9.

29. Dogruca Z, Kabasakal L, Yapar F, Nisil C, Vural VA, Onsel Q. A comparison of Tl-201 stress-reinjection-prone SPECT and Tc-99m-sestamibi gated SPECT in the differentiation of inferior wall defects from artifacts. Nucl Med Commun 2000;21:719–27.

30. Ficaro EP, Fessler JA, Shreve PD, Kritzman JN, Rose PA, Corbett JR. Simultaneous transmission/emission myocardial perfusion tomography. Diagnostic accuracy of attenuation-corrected 99mTc-sestamibi single-photon emission computed tomography. Circulation 1996;93:463–73.

31. Picano E, Sicari R, Landi P, et al. Prognostic value of myocardial viability in medically treated patients with global left ventricular dysfunction early after an acute uncomplicated myocardial infarction: a dobutamine stress echocardiographic study. Circulation 1998;98:1078–84.

32. Previtali M, Fetiveau R, Lanzarini L, Cavalotti C, Klersy C. Prognostic value of myocardial viability and ischemia detected by dobutamine stress echocardiography early after acute myocardial infarction treated with thrombolysis. J Am Coll Cardiol 1998;32:380–6.

33. O'Connor MK, Gibbons RJ, Juni JE, O'Keefe J Jr., Ali A. Quantitative myocardial SPECT for infarct sizing: feasibility of a multicenter trial evaluated using a cardiac phantom. J Nucl Med 1995;36:1130–6.

34. Choi KM, Kim RJ, Gubernikoff G, Vargas JD, Parker M, Judd RM. Transmural extent of acute myocardial infarction predicts long-term improvement in contractile function. Circulation 2001;104:1101–7.

35. Wu KC, Zerhouni EA, Judd RM, et al. Prognostic significance of microvascular obstruction by magnetic resonance imaging in patients with acute myocardial infarction. Circulation 1998;97:765–72.

36. Klem I, Heitner JF, Shah DJ, et al. Improved detection of coronary artery disease by stress perfusion cardiovascular magnetic resonance with the use of delayed enhancement infarction imaging. J Am Coll Cardiol 2006;47:1630–8.

37. Amado LC, Gerber BL, Gupta SN, et al. Accurate and objective infarct sizing by contrast-enhanced magnetic resonance imaging in a canine myocardial infarction model. J Am Coll Cardiol 2004;44:2383–9.

38. Simonetti OP, Kim RJ, Fieno DS, et al. An improved MR imaging technique for the visualization of myocardial infarction. Radiology 2001;218:215–23.